Acta Materialia 53(18), 4903–4917 (2005)

Lead and lead alloy foams

Andree Irretier[1♦] and **John Banhart**[2♦]

[1]Institut für Werkstofftechnik, 28359 Bremen, Germany

[2]Hahn-Meitner-Institut and Technical University Berlin, 14109 Berlin, Germany

[♦]formerly at: Fraunhofer-Institute for Advanced Materials, 28359 Bremen, Germany

Lead-based foams were produced by applying the powder route, i.e. by mixing metal powders and a powdered gas-releasing blowing agent and pressing the mixture to a foamable precursor material after. This precursor was then foamed by heating it up to above its melting point, thus triggering gas release and foam formation. In a first step a set of process parameters was established, allowing us to foam lead alloys. This included finding suitable metal and blowing agent powders, mixing and compaction procedures, and to determine appropriate foaming conditions. After this the foaming process of various alloys was studied as a function of time, temperature, alloy composition and blowing agent content.

Keywords:

1. powder processing	2. foaming
3. lead	4. foams

1 Introduction

Cellular metals can be produced by a variety of different methods [1]. A versatile and promising method for producing closed-cell metal foams from metal powders was rediscovered in the early 1990s [2] after it had been developed long ago [3]. The process comprises mixing metal powders and a powdered blowing agent and compacting the mix to a dense semi-finished product (called „foamable precursor material“) by hot pressing, extrusion, powder rolling or other methods. In the actual foaming step the foamable precursor material is expanded by heating it up to above its melting point. This transfers the metal into a semi-liquid viscous state and simultaneously makes the blowing agent decompose, thus releasing gas and creating a highly porous structure [4].

Up to now the main focus in the literature has been on aluminium and aluminium alloy foams [5][6]. The present paper deals with lead and lead alloy foams. There is some technological interest in lead foams because of possible applications: they could, e.g., be used as light-weight electrodes in lead-acid batteries. As lead foams are superconducting below 7 K, their use as cryogenic shielding material has been proposed [7]. Furthermore, lead foams are interesting because they allow us to study foaming processes in metals fairly easily at low temperatures. As lead has a high density of 11.34 g/cm^3, such foams are being used for comparative studies of foams under normal and zero gravity conditions, e.g., for studying drainage phenomena [8].

To be able to produce high-quality lead foams the process parameters have to be chosen carefully. This includes an appropriate selection of the metal powders, the alloy composition, the type of blowing agent, compaction conditions and, finally, foaming temperatures. Establishing these parameters was one purpose of the present work. We succeeded in creating uniform lead foams with densities as low as 1 g/cm^3 using pure lead powder to which basic lead carbonate was added as a blowing agent. The decomposition range of this blowing agent fits to the melting point of lead. Moreover, by using a lead compound as blowing agent one can avoid adding further metals which could be a useful property in some electrochemical applications where contaminations can be deleterious [9]. An example for such a foam can be seen in Figure 1. This foam was later used as test material in a battery test.

Lead alloys were also considered. Tin and antimony are the most important alloying elements of lead. Both lower the melting temperature of lead and therefore modify foaming conditions. Moreover, these alloying elements improve mechanical properties

[10] which might be important for foam applications.

In addition to technological development it is important to improve knowledge about the physics of foaming of metals. We therefore investigated the foaming process of lead alloys as a function of time and temperature in a quantitative way and analysed both the kinetics of foaming and the structure of the resulting foams. Alloy composition and blowing agent content were varied which allows to draw conclusions about the mechanisms governing foaming.

The paper is organised as follows: Sec. 2 describes the parameter optimisation process which finally led to a formulation yielding lead alloy foams of good quality. After a description of experimental techniques in Sec. 3, Sec. 4 then contains some investigations of the foaming behaviour of lead alloys based on the optimal procedure. Is it inevitable that the search for good processing parameters implies some preliminary interpretation which has to be given already in Sec. 2. However, the final discussion and conclusions are presented in Sec. 5 in the light of all experiments.

2 Establishment of process parameters

A first task was to establish an experimental procedure for producing stable lead foams. Preliminary experiments failed in which aluminium powder was simply replaced by lead and pressing temperatures were reduced accordingly, while otherwise the same blowing agents and pressing procedures known for aluminium alloys were applied. The resulting compacted precursor material could not be foamed by melting. It became clear that the selection of both metal powder and blowing agent and also the choice of a suitable compaction method and the associated adjustment of pressing parameters had to be carried out newly for lead. Experience with foaming aluminium alloys, however, was useful since it helped us in pre-selecting promising process parameter combinations.

2.1 Variation of materials and process parameters

2.1.1 Metal powder

Twelve different lead powders were purchased covering a variety of product types, nominal powder size ranges and purities. Size distributions and oxide contents were determined by laser particle size analysis (Coulter LPA) and hot gas extraction (LECO TC436), respectively. The parameters characterising these powders as given by the manufacturer and as measured by us are given in Table 1. The measured oxygen content has been converted to a volume content of the oxide PbO which is stable at high temperatures

(density: 9.64 g/cm^3 [11]) because this property is actually more meaningful in the context of foam stabilisation. This PbO content ranges from 1 to 65 vol% for the different powders.

In a second step tin (Alfa Aesar, <150 μm, purity 99.5%) or/and antimony powder (Chempur, <100 μm, purity 99%) were added to the lead powder to create binary or ternary alloys from these simple eutectic systems.

2.1.2 Blowing agent

The temperature range in which a blowing agent releases gas has to match the melting range of the alloy to be foamed [12]. As the precise decomposition behaviour of inorganic substances is not always known and also might be influenced by the compaction process and the surrounding metallic matrix we chose a variety of hydrides (Mg-, Ti-, Zr-) and carbonates (Cu-, Mg, Zn-, Pb-) and carried out trial experiments.

2.1.3 Mixing of powders

Metal and blowing agent powders were mixed in a tumbling mixer for 30 minutes. Quite frequently agglomeration of the very fine carbonate particles (see Figure 2a) was observed. Adding steel balls to the mixing container helped in improving the results. The quality of mixing was checked by visual inspection which was facilitated by the difference in colour between the powders (lead powders are dark grey, most carbonates white). The absence of visible clusters of carbonate was interpreted as a good result. A microscopic view of such a good mixture (Figure 2b) shows large lead particles covered with very fine $(PbCO_3)_2{\cdot}Pb(OH)_2$ particles. The tin particles are seen as small spheroid particle in between. Such mixtures proved to be well compactable and to yield good foams in some cases. No further optimisation of powder mixing was carried out for this reason.

2.1.4 Compaction of powder mixtures

A simple and often used method for the compaction of powder mixtures to dense precursors is hot pressing. Therefore, the first experiments for making foamable lead precursors were carried out in a hot pressing tool. Powder mixtures of pure lead (m.p. 327°C) and blowing agent were compacted at 250°C and a pressure of 110 MPa for 20 minutes. Tablets with 29 mm diameter and 8 mm height were obtained.

After it was realised that hot pressing did not yield useful results (see 2.2.1) we constructed an extrusion tool aiming at creating a higher degree of shear in the material. This is thought to improve bonding between the individual particles during material flow and to avoid the problems encountered with hot pressed powders. As shown in Figure 3 the tool

consists of a vertically arranged cylindrical die which can be closed at the bottom and which has a round bore of 8 mm diameter at the side. The die was filled with 350 g of lead powder mixture, after which the ram was inserted and the powder was pre-compacted at 20 kN and room temperature. The bore hole was closed with a thin aluminium foil at this stage. The filled die was then pre-heated to 275°C and held for 2 hours after which final pressing was initiated. As soon as the force exceeded about 100 kN the metal started to flow and a compact wire was extruded at a rate of about 10 mm/sec. We call this procedure *transverse extrusion*. The extrusion ratio was 1:14 in the present case.

2.1.5 Foaming

Simple free-foaming experiments were used for the characterisation of foamability. A furnace was pre-heated to and held at a given temperature. A copper sheet was used as a substrate for foaming. Pieces of compacted precursor material were placed on the pre-heated sheet. The foaming process was observed visually through a window in the furnace. After maximum expansion was reached the foam was taken out of the furnace, cooled with a ventilator and allowed to solidify. Furnace temperatures ranged from 350°C to 550°C.

2.2 Influence of various parameters on foam quality

We shall now review the results of parameter optimisation starting with the most important step, namely powder consolidation.

2.2.1 Powder compaction

Hot-pressed tablets were heated in a furnace set to 450°C. We observed melting of the precursor and the occurrence of melted droplets on the surface of the precursor but no foaming as can be seen in Figure 4. We could not achieve any satisfactory foaming for a variety of different powders, blowing agents and pressing parameters. We suspect that the densification of powders was not sufficient to shear off the oxide layers from the individual particles and to create a metallic bonding and a gas-tight structure. Instead the liquid was squeezed out by the evolving gas and no bubbles were formed.

Extrusion as described in Sec. 2.1.4 immediately led to very promising results. Most extruded precursors showed quite some degree of foam expansion. No melt droplets are formed at the surface in most cases. Expansion is smooth and the achievable expansion factors exceeded 11 in the best cases. Many of the foams had a uniform pore structure such as the one shown in Figure 1. For this reason we did not carry out any further optimization of powder consolidation. Relative densities of the extruded bars were above 98.2% for pure lead

and above 96.6% for all the alloys investigated. There is no clear dependence of the final density on alloy composition.

2.2.2 Blowing agent

We obtained the best results using lead carbonate with the nominal composition $(PbCO_3)_2 \cdot Pb(OH)_2$ (99%, Alfa Products). This carbonate is called *basic lead carbonate* or *white lead*. Its mean particle size was determined by laser particle analysis. However, the value of 11 μm which was obtained does not seem to represent the true particle size if one compares it to the apparent size of most particles in Figure 2a. This is an indication of strong agglomeration which was not removed even by the ultrasound-assisted dispersion in the particle analyser.

Use of $(PbCO_3)_2 \cdot Pb(OH)_2$ led to said volume expansion factures up to 11. The blowing agent content was varied from 0.5 to 3 wt.%. It was found that increasing blowing agent contents exacerbate the problems with mixing and compaction. 2 wt.% were chosen as a good compromise. Surprisingly a similar water-free carbonate $PbCO_3$ did not lead to good foam expansions. Second best was MgH_2, yielding a volume expansion factor of slightly above 2.

2.2.3 Foaming temperature

Furnace temperature clearly influences foaming as we know from aluminium foams [13]. Lower foaming temperatures prolong the time needed to reach the melting range and also reduce the degree of final foam expansion because during slow heating gas can escape from the expanding precursor without creating pores. Figure 5 shows samples foamed at two different temperatures. A pronounced difference in foam expansion can be noticed. Above 500°C foam expansion tends to reach a limit while oxidation becomes very strong. 450°C was therefore taken as a “standard temperature” for comparative tests. The foaming process is very fast at this temperature. After the onset of melting foam expansion up to the maximum volume can take place in the order of 10 s depending on sample size.

2.2.4 Metal powder

To be able to assess the suitability of a given lead powder we defined an evaluation system for the resulting foams [14]. Four properties were evaluated and 0 to 3 points given for each property, each weighted by a factor expressing the importance we assign to this property guided by our experience. The points were then summed up to yield a final quality number (see Table 2), the highest possible value of this number being 30. The percentage of these 30 points which was actually reached for a given lead powder is called *foaminess* and is given in

Table 1 for all the materials considered. We found that the most important parameters influencing foamability were oxygen content and powder size. The best results were obtained using a powder from Cerac-Chemco with an average particle size of 82 μm (90 vol.% > 50 μm, d_{50}=80 μm, 90 vol.% < 141 μm). This powder reached 28 points, e.g. 93% of the possible 30 points. It had good flow properties, a fairly light grey colour and did not agglomerate. The oxygen content of the freshly obtained powder packed under argon was 0.12 wt.%. After being stored in a glass container under air the original content increased up to 0.16 wt.% after one week. Six months after the measurements the powder was characterised once more and then had an oxygen content of 0.37 wt.% [15]. Figure 6b shows an example for a foam based on this powder.

Powders which did not lead to good foaming fall into two categories. The first includes powders with a high oxygen content up to 4 wt.% which did not flow well and had a lumpy consistency and a dark grey or even reddish colour. The extruded precursor did not foam well and showed a similar behaviour already observed for hot-pressed tablets, i.e. the formation of melt droplets at the surface. These powders obtained only 20% of the possible points. Figure 6c shows an example for a “foam” made from these materials.

Powders with a very low oxygen content down to 0.06 wt.% were spherical and quite coarse. They were easy to compact and showed some foaming. However, the foams were not stable. Strong drainage occurred during foaming and a pool of liquid metal emerged at the bottom of the foam. 30-50% of the possible assessment points confirmed the inferiority of these powders. Figure 6a shows a foam made with one such powder.

As the oxygen content of lead changes gradually during exposition to air due to reactions with O_2 or CO_2 we checked for possible changes during processing. Lead powder without lead carbonate additions was moved in the mixer and then extruded. The oxygen contents of the starting powder, the “mixed” powder and the extruded bar were then measured. We found the same value for all samples within a limit of 20%. Therefore, the oxygen content remains nearly constant during processing. Long exposure to air at room temperature, however, leads to progressive oxidation or carbonate formation as mentioned above.

2.2.5 Alloy composition

In order to tailor foam properties tin and antimony were added to the lead powder. Processing parameters were not changed except that the pressing temperature was adapted to the lower melting temperatures of the Pb-Sn , Pb-Sb and Pb-Sb-Sn alloys. It was ensured that

the pressing temperature was well below the solidus temperature of the alloy processed and below the lowest melting point of any of the elementary component as we are processing powder mixtures. Alloys with up to 30 wt.% Sn and up to 10 wt.% Sb and a ternary alloy containing 10 wt.% Sn and Sb were successfully processed to foams. Precursors containing Sb were quite hard and difficult to cold-roll, alloys containing Sn very soft. The foaming behaviour of these alloys will be described in Sec. 4 in a quantitative way.

3 Sample preparation and foam characterisation technique

3.1 Manufacture of foamable precursor for foaming tests

Powder mixtures reflecting the composition of pure lead and the alloys Pb-Sn (5, 10, 30 wt.% Sn), Pb-Sb (3 and 10 wt.% Sb) and PbSb10Sn10 were processed to 8 mm thick wires by transverse extrusion. Some of these wires were cold-rolled to 1.2 mm thickness and then cut to square pieces 35×16 mm^2 in size to be used in free-foaming experiments.

3.2 Free-foaming experiments and foam characterisation

In order to determine the evolution of pore structure during the foaming of lead alloys, so-called “free-foaming” experiments were carried out. The procedure was similar to that described in Sec. 2.1.5. Samples prepared by rolling were placed onto a pre-heated substrate and were allowed to foam for a given time after which the foaming process was interrupted by air quenching. The densities ρ of the foamed samples were determined by buoyancy measurements. The foams were then sectioned and analysed. For this the specimens were embedded in a white resin and polished with a grid 800 paste. This led to a clear contrast between cell walls and voids. Images were scanned and analysed quantitatively using the computer programme “Optimas 6”. In some cases artefacts stemming from cell walls interrupted by polishing or by pieces of resin fallen out of small pores had to be corrected manually. Pore size distributions and the mean apparent pore diameter d were derived by the computer program. As quantitative analysis of very small pores turned out to be unreliable we only took account of pores with a diameter above 0.5 mm. This of course limits the significance of the mean value d. Whenever d is close to 0.5 mm the calculated d is systematically larger than the true average including all pores. We therefore overestimate d for foams with a fine porosity and therefore cannot use d as an absolute measure but rather as a qualitative indicator for pore size.

3.3 Foaming experiments in expandometer

Free-foaming experiments yield quick information about the overall expansion behaviour, but a precise picture especially of the early expansion stages requires a

quantitative in-situ characterisation method of expansion as provided by the so-called *expandometer*. The set-up of the expandometer is shown in Figure 7. The furnace (not shown) heats a foamable sample (2) placed in a cylindrical mould (1) allowing for vertical expansion only. The mould is mounted on a fixed support (7). Expansion is monitored by a dual position sensor (3,4) measuring the difference between the position of the upper piston relative to the sample substrate and thus compensating for most of the thermal expansion effects in the experimental set-up not stemming from the sample. Both sample and furnace temperatures are measured with thermocouples (5,6). A discussion of the expandometer can be found in Ref. [13]. It was found that the weight of the piston has little effect on foam expansion in a way that final expansion is only marginally larger in free-foaming experiments than in expandometer tests. Foam evolution can be monitored in a reliable way for the expansion phase, while the collapse phase is often disturbed by frictional effects between piston and tube.

Specimens for foaming were obtained by cutting small chips off a piece of extruded precursor wire and compacting them at 200 kN to cylindrical tablets of 29 mm diameter (at room temperature). Direct hot pressing of powders to tablets was not possible due to the limitations described in Sec. 2.1.1. For each parameter set two specimens were characterised.

3.4 Thermoanalysis

A Netzsch 409C STA (Simultaneous Thermal Analyser) was used to measure heat flow and mass change during continuous heating of blowing agent powder. The heating rate was 10 K/min and the argon flow rate 50 ml/minute. 100 mg of powder were characterised in alumina crucibles in each experiment.

4 Results

In this section we describe investigations related to the foaming process of lead and lead alloys. After an analysis of the blowing agent and the foamable precursor the expansion kinetics of foaming lead alloys are investigated either in free-foaming experiments or in the expandometer.

4.1 Thermo-analysis of blowing agent

Figure 8 shows thermo-analytical data for $(PbCO_3)_2 \cdot Pb(OH)_2$. In the DSC trace we can distinguish two distinct decomposition stages, marked “I” and “II”. The first takes place from about 266°C (determined by the tangent method) to a maximum around 309°C, the second from 323°C to 359°C. In addition, there is a small endothermal reaction below 100°C.

Corresponding to the DSC trace the mass loss also takes place in two stages as can be seen best by considering the derivative of the TGA curve which matches the DSC trace very well. The first peak of this mass change curve is more pronounced with an area 2.25 times that of the second. Therefore, main gas evolution occurs slightly below the melting point of pure lead which is indicated in Figure 8 as a short vertical line. The lead alloys investigated have melting ranges which are below the maximum of the first decomposition peak but still fall into the decomposition range.

4.2 Microstructure of precursor material

Figure 9 shows cut sections of two foamable lead alloy precursors after rolling. Polishing the soft lead specimens turned out to be difficult. Especially for PbSb10 the integrity of the rolled material was not sufficient to maintain a dense matrix. Particles fell out of the surface to be prepared leading to quite some porosity (see Figure 9b). Therefore the samples could not be fully polished to reveal microstructural details in depth. What is clearly discernible is that Sb particles embedded in lead maintain their shape even after rolling, whereas Sn particles are largely elongated in the rolled state (see Figure 9a). The Pb-Sn system was less prone to the difficulties encountered with Pb-Sb and showed a better structural integrity and consequently fewer pores.

4.3 Free-foaming of lead and lead alloys

4.3.1 Influence of foaming time and alloy composition

Figure 10 compares the density variation with foaming time for different lead and lead alloy foams. Here foaming time means the time elapsed between the first contact of the foamable precursor with the sample substrate and the initiation of sample cooling. The time span shown in Figure 10 ranges from 10 to 60 s. Shorter foaming times were difficult to control and were therefore not considered. The density drops during the expansion phase of the foam, reaches a minimum and then either stays constant or rises again indicating some foam collapse. Obviously foaming is a strongly non-linear process. In the first ten seconds not resolved here most of the expansion takes place. After 60 s the changes are quite small. Pure lead reaches a minimum density after about 20 s and is quite stable after. Additions of antimony lead to both a higher minimum density and a more pronounced collapse after maximum expansion. This effect is stronger for 10% Sb than for 3%. Additions of tin, on the other hand, enhance foaming and not only produce lower final densities but also reduce collapse. After maximum expansion density remains almost constant up to the longest foaming time. The ternary alloy PbSb10Sn10 behaves very much like binary Pb-Sn alloys.

The evolution of pore structure during foaming can be monitored by comparing sections of samples foamed for different times. Figure 11 shows a series of such images for the PbSb10Sn10 alloy. Corresponding to volume expansion, the density ρ decreases with foaming time while the average equivalent pore size *d* increases. The distribution of pore sizes and shapes in the foams is quite irregular, especially for the longer foaming times where many small pores co-exist with only a few large pores with diameters up to 4 mm. The mean apparent pore diameter *d* ranges from 0.7 to 0.95 during the time interval considered. The true change in pore size is underestimated by our analysis as explained in Sec. 3.2.

4.3.2 Influence of blowing agent content

A series of different alloys containing either 0.5 or 2 wt.% blowing agent $(PbCO_3)_2 \cdot Pb(OH)_2$ was foamed at 450°C. Foaming times ranged from 10 to 60 s. The densities of the resulting foams are shown in Figure 12 as a function of time.

Foam expansion - reflected by lower foam densities - is much stronger for the higher content of blowing agent. Moreover, expansion is faster. Alloys containing 2% blowing agent complete their expansion after 12-20 seconds and reach minimum densities below 1 g/cm^3 for fully expanded PbSn5 and PbSn10 alloys. Foams with 0.5% blowing agent continue expanding slowly even after 30 s (except for PbSb3 where they collapse). Pure lead does not reach densities below 2.4 g/cm^3 even after 60 s of foaming. PbSb3 expands quickly up to a minimum density of 2.3 g/cm^3 but then collapses. Only the alloys containing tin reach lower densities around 1.7 g/cm^3 and appear stable within the first 60 s.

Images of foams based on pure lead and two Pb-Sn alloys after 60 s of heating are compared in Figure 13. For the foams blown with 2% blowing agent cells are more expanded. Densities are between 40 and 55% lower than for 0.5% blowing agent. There is also a marked difference in pore size. 2% blowing agent content produces quite a number of large cells and an average cell size *d* which is nominally 33 and 64 % higher than for 0.5% blowing agent content. This difference is even larger in reality as explained in Sec. 3.2 since *d* for the foams made with 0.5% blowing agent is quite close to the cut-off size of 0.5 mm in our analysis.

4.3.3 Influence of foaming temperature

Figure 14 gives the density evolution of various lead alloy foams for a lower foaming temperature than that in Figure 10, namely 400°C. Obviously, foaming is slower for 400°C than for 450°C. At a given time, e.g. 12 s, densities are higher for most alloys than the densities reached at 450°C. Densities corresponding to maximum expansion, however, are

only slightly higher for 400°C. One difference is stability of some of the foams: Foaming at the lower temperature slightly reduces the degree of collapse of the two Pb-Sb alloys.

Figure 15 shows the influence of foaming temperature on a) pore size, and b) density. A constant foaming time of 16 s was chosen, because at this time most foams shown were still quite stable and little collapse had occurred. Pb-Sb foams were not included in Figure 15a since they exhibit very pronounced collapse phenomena at higher temperatures (even more than the collapse shown in Figure 10 and Figure 12). Pore size values obtained for these alloys showed an erratic behaviour so that merely their density is given in Figure 15b. A first observation is that higher foaming temperatures lead to larger pore sizes for all except one data point. Moreover, there is a clear dependence of pore size evolution on alloy content. Pure lead develops the coarsest pore structure. Increasing tin contents leads to smaller pores. The ternary alloy PbSb10Sn10 lies between PbSn10 and PbSn30.

The average densities of the foams, see Figure 15b, show a pronounced dependence on temperature too. All samples expect PbSb3 and PbSn5 exhibit a density minimum between 450 and 500°C. The lowest density of all samples is found for PbSb10Sn10 foamed at 500°C. This foam not only has a fine pore structure but also a density of only 0.93 g/cm^3, which corresponds to an expansion factor of 12.2.

4.4 Expandometer foaming

4.4.1 Influence of sample thickness

In a first step we determined the influence of sample dimensions on the foaming behaviour of pure lead precursors. In Figure 16 the expansion kinetics of pure lead foams and the corresponding sample temperatures are displayed. Expansion is given as $\eta = V/V_0$, where V is the current foam volume, V_0 the volume of the unfoamed precursor. All samples were cylindrical, with a constant diameter of 29 mm, but sample height was varied. The temperature curves show that the heating rate in the thinnest sample is highest, followed by the thicker specimens. In all cases the arrest point during heating is close to 327°C which is the melting point of lead. After melting the temperature in the samples further rises and approaches the furnace temperature. The corresponding expansion curves show that the thinnest sample starts to expand first, while expansion of the thicker specimens is delayed, reflecting delayed heating. Foaming starts as soon as the melting point of lead has been reached. The overall foaming course is the same in all three cases. A maximum of foaming is observed at about 350°C after which a regime of collapse follows. Collapse is more pronounced in the expandometer than in free-foaming under equal conditions (compare to

Figure 10). The thicker sample reaches a lower maximum expansion which can easily be attributed to the higher sample mass resting on the expanding foam and hindering expansion. The two thinner samples, however, are not too different concerning their maximum expansion. Therefore it can be concluded that precursor thicknesses up to 6 mm lead to the same results and 6 mm was selected as standard thickness for all the expandometer experiments. This corresponds to a sample weight of about 40 g.

4.4.2 Influence of alloy composition

The foaming behaviour of some Pb-Sn and one ternary alloy was compared to pure lead in a series of expandometer experiments. Figure 17 shows the corresponding expansion diagrammes. Obviously, addition of tin shifts the onset of foaming to earlier times by 100 s in Figure 17a. In addition, maximum foam expansion increases with tin content, a notable increase being observed for 10% Sn or more. All foams show some collapse after maximum expansion. The ternary alloy PbSb10Sn10 expands slightly more than PnSn10 but foam collapse is a bit more pronounced. In contrast to alloys containing Sn, alloys with Sb (Figure 17b) exhibit slightly lower maximum expansions than pure lead while foam collapse appears more pronounced. The onset of foaming is also shifted to earlier times by Sb additions.

Analysing the temperature at which foam expansion begins – defined as the point at which expansion reaches 1% of maximum expansion – we find that pure lead starts at 327°C which is exactly its melting point. Additions of Sb lower the onset of expansion to about 305°C almost independently of concentration. Additions of Sn, on the other hand, lead to an onset temperature around 250°C without much dependence on tin concentration. The same applies to the ternary alloy PbSb10Sn10 which starts at 251°C.

5 Discussion

5.1 Metal powder properties

The experience that successful foaming of lead alloys requires powder compaction by transverse extrusion and the found sensitivity of foaming behaviour on powder properties shows that the surfaces of the powder particles, namely, the oxide or carbonate layers on individual particles play a very important role. During compaction of metal powder mixtures the oxide layer of each individual powder particle has to be sheared off to allow for the creation of a metallic bonding between neighbouring powder particles and to ensure that blowing agent particles are enclosed in a dense metallic matrix. Hot compaction – sufficient for making foamable precursors from aluminium alloys – does not provide enough shear to densify lead powders, at least not the commercial powders used. As a consequence gas

escapes from the precursor without creating bubbles and merely pushes out some of the liquid during heating. This gives rise to the often observed droplets as shown in Figure 4. For too high oxide contents even transverse extrusion is not sufficient to break up the oxide layers and no foamability can be achieved at all (Figure 6c).

Reducing the oxygen content to a very low level is not a good strategy to improve this situation since, on the other hand, a certain oxide content is necessary to ensure foam stability as shown in Figure 6. It is well known that metal foams are stabilised by solid particles floating in the melt [17][18][19], a phenomenon which is also known from aqueous foams and emulsions [20]. Wübben could recently show [15] that the ratio between the total internal pore surface of a lead foam is proportional to the volume content of the entrained oxide and concluded that the oxides float on the foam films during foaming and create stabilisation by a still disputed mechanism [21]. Consequently, a too low oxide content leads to coarsening until the pore surface area has adjusted to the available amount of oxide.

The best choice of lead powder is a compromise between various requirements. This is reflected by the properties of our best powder, a medium coarse powder of 82 μm mean particle size and a medium oxygen content, i.e. in the order of 0.2 wt.%, corresponding to 3 vol.% PbO. From the difficulties encountered it becomes clear that metal powder properties play a more important role for lead than for aluminium in a sense that the quality of the emerging foam depends sensitively on the nature of the powder used.

Aluminium foams contain about 1 vol.% Al_2O_3 which is sufficient to stabilise the films [13][22]. Therefore the oxide content in lead foams is higher than in aluminium but has the same order of magnitude. We therefore assume that the basic stabilisation mechanism is the same. In addition to the oxides originating from the former powder surfaces one has to take account of the residues from the blowing agent which are present in lead foams (lead oxide) and aluminium foams (titanium or titanium oxide). These residues could also contribute to stabilisation, although their effectivity is probably low because these particles are quite coarse compared with the submicrometre size of the oxides present in the precursor.

Addition of alloying elements has an important impact on both structure and properties of the precursor. The differences observed between Sn and Sb are mainly due to the difference in hardness of these elements. The Brinell hardness 3.9 of tin is just slightly higher than that of Pb (2.4), whereas Sb has a much higher hardness above 30 [23]. This explains why only tin particles are deformed during extrusion, whereas Sb particles remain

unchanged. The intense and simultaneous deformation of both tin and lead can be thought to yield the better structural integrity observed for extruded wires made from Pb-Sn alloys.

5.2 Blowing agent

In order to ensure good foaming the decomposition characteristics of the blowing agent have to match the melting range of the alloys to be foamed [12]. Titanium and zirconium hydrides successfully used for foaming Al or Zn alloys did not yield good results because their main decomposition takes place above about 400°C [24][25]. The decomposition behaviour of the most suitable blowing agent found in this study as shown in Figure 8 clearly meets the requirements more than these hydrides. However, the reason why MgH_2 and other carbonates studied led to inferior results, although their decomposition takes place in the required temperature range, is not entirely clear. It has to be assumed that beside the temperature dependence of gas release from loose powder other factors play a role such as the way the blowing agent particles are embedded in the metallic matrix during extrusion. This might depend on morphological properties of the powder particles and give rise to a different residual porosity or structural integrity of the precursor which in turn influences foaming.

Given the decomposition reaction of the blowing agent and the known molar weights of the components involved:

	$(PbCO_3)_2 \cdot Pb(OH)_2$	$\rightarrow 3PbO$	$+ 2CO_2\nearrow$	$+ H_2O\nearrow$
molar weight:	776	670	88	18

we can calculate the weight reduction of the precursor after total decomposition. This theoretical reduction is -13.7% which roughly corresponds to the measured mass decrease of −16.5 % (see Figure 8).

We can calculate the maximum gas volume which can be released from a given volume of foamable precursor. Accordingly, 1 cm^3 of precursor containing x wt.% of $(PbCO_3)_2 \cdot Pb(OH)_2$ releases $7.5/x$ cm^3/wt.% of water and $15/x$ cm^3/wt.% of CO_2 at the m.p. of lead (327°C). In order to achieve a maximum expansion factor of, e.g., 11 which is actually observed when foaming precursors containing 2 wt.% blowing agent (corresponding to a final foam density of 1 g/cm^3) one would need 10 cm^3 of gas from each cm^3 of precursor. If water and CO_2 acted in the same way and no gas were lost, a blowing agent content of $x = 10/(7.5+15) \approx 0.45$ wt.% should yield this expansion factor. In reality we observe that no full expansion is reached at this level of blowing agent as can seen from Figure 12. Therefore,

either gas is lost during foaming and/or decomposition is incomplete at the temperatures applied. Figure 8 actually shows that only about 2/3 of the total gas amount is released at the m.p. of lead and even less for lead alloys. Therefore gas losses can be inferred which is plausible since the precursor is not totally dense and the surface of the emerging foam is rough and contains holes (Figure 5). A blowing agent content of 2 wt.% seems to be the ideal choice both from the theoretical and the experimental viewpoint.

Increasing the blowing agent content beyond the level of 2 wt.% created problems with mixing and compaction as pointed out already. Even if it were possible to use more blowing agent it is not sure whether this would lead to lower densities. Comparing foaming for two different blowing agent contents in Figure 12 we see that maximum expansion is not four times higher for 2% compared to 0.5%. In aluminium foams expansion does not further increase beyond a certain level (about a factor 5 for a common alloy such as AlSi7) if the blowing agent content is increased [26]. Instead, cells coalesce as films are overstretched and the foam is prone to collapse [27]. Figure 13 shows that pore morphologies depend very much on the blowing agent content. The higher content of 2 wt.% leads to a lower final density after 60 s of foaming but at the cost of a more heterogeneous pore structure. Obviously the stronger expansion has triggered rupture events, a phenomenon called growth coalescence by Körner et al., who showed that density and pore size are correlated

[28]. Our data does not show this clear correlation - perhaps due to the low precision of pore size measurement – but it shows the existence of this effect.

5.3 Foaming process

The time dependence of foam expansion as expressed by the expandometer tests looks very much like that of aluminium alloys (compare expansion diagrams, e.g. in Figure 17, with those in Ref. [13]). Foam expansion starts as soon as an internal gas pressure is building up and enough liquid is available to allow for the evolution of liquid films. As the furnace temperature lies above the liquidus temperature of the alloy to be foamed, there is always some overheating in late stages of foam expansion and correspondingly collapse phenomena are observed. The evolution of pore structure as seen in Figure 11 also resembles that of aluminium. We observe a growth in size and a reduction in number of cells, i.e. coalescence driven by expansion.

The various foaming experiments show that the foaming behaviour of lead alloys depends on the same parameters known from foaming aluminium, namely foaming temperature and alloy composition.

Foaming **temperature** influences both foaming kinetics and expansion behaviour. Obviously, higher foaming temperatures lead to faster heating up to the melting temperature, more efficient heat transfer into the melting material and therefore earlier foaming. A comparison between Figure 10 and Figure 14 shows this very clearly. At higher temperatures, i.e. at T≥500°C, higher foam expansions can be achieved compared to low temperatures if foaming is stopped at maximum expansion as demonstrated in Figure 5. For lower temperature, however, the difference is quite small (compare 400 and 450°C in Figure 10 and Figure 14). For a fixed foaming time – e.g. 16 s – the picture is more complex (see Figure 15b). Here the lowest densities are achieved at intermediary temperatures for most alloys. This means that an increase in temperature first leads to a higher volume expansion (except for PbSn5 and expecially PbSb3), later to a reduction in expansion (all alloys). Therefore an optimum temperature for highest foam expansion exists at a given time. Higher temperatures than this optimum lead to a more pronounced foam collapse and higher densities, lower temperatures to retarded or incomplete foaming. The temperature dependence of collapse is seen best for Pb-Sb alloys in Figure 10 and Figure 14. These figures show a certain degree of collapse after maximum expansion in all cases, but collapse is much stronger for 450°C than for 400°C. The reason for this must be the lower viscosity of melts at higher temperatures which lead to instable foams if foam stabilisation is insufficient. Higher temperatures also lead to coarser pore structures for all alloys as demonstrated in Figure 15a. At higher temperatures (i.e. T≥500°C) pores become larger although density increases. This is another indication for an increasing rate of coalescence in the foam at higher temperatures.

The various **alloys** investigated behave in quite a different way. Taking pure lead as a reference system additions of tin and antimony were investigated. Both lower the melting temperature. Consequently, foaming starts earlier as can be seen best from the expandometer measurements in Figure 17. However, the action of Sn and Sb is quite different. Sn improves foaming, i.e. leads to higher expansions, more stable foams and also to finer pore structures (see Figure 15a), whereas Sb leads to poorer foaming, i.e. foam expansions are lower and fully expanded foams show a pronounced collapse. Note that the expandometer tests in general show more foam collapse than free-foaming experiments which can be attributed to the weight of the piston.

As both Sn and Sb lower the melting point of lead the change in foamability upon alloying cannot be an effect of melting temperature alone. The processes during melting of Pb-Sn and Pb-Sb must be responsible for the difference. As the ternary alloy PbSb10Sn10 shows the favourable behaviour of binary Pb-Sn alloys a beneficial action of Sn can be inferred. We think that the low melting point of tin at 232°C in contrast to antimony which melts at 631°C is responsible for the difference. While heating up foamable Pb-Sn or Pb-Sb-Sn precursors (which are heterogeneous mixtures of elementary powders) some metallic melt is formed in a very early stage. This will certainly speed up the alloying process and also close the network of pressing porosity in the precursor through which part of the blowing gas can escape. In Pb-Sb the Sb powder particles remain solid until diffusion across the interfaces between Pb and Sb creates some eutectic liquid. As heating rates are very fast in our experiments this is not expected to happen below the melting point of lead at 327°C. Therefore only alloys containing elementary tin show this behaviour which is known to assist foaming, namely the early formation of liquid, while Pb-Sb alloys do not.

Another possible reason for the different foaming behaviour of Pb-Sn and Pb-Sb might be the different consistency of the precursor as seen from the micrographs in Figure 9. The addition of soft tin particles yields a precursor which has a high structural integrity, whereas additions of antimony do not. As a consequence, during foaming of Pb-Sb more internal de-bonding occurs which facilitates the escape of blowing. Finally, one could also speculate that the melt properties of Pb-Sn and Pb-Sb are different, e.g., the value for viscosity or the proneness to gas-metal reactions with CO_2 or O_2 in the different alloys which could also influence the foaming process. However, the explanation given above seems more likely since the ternary system behaves like binary Pb-Sn alloys.

6 Conclusions

- Lead and lead alloy foams could be produced by modifying the powder compact process known for aluminium alloys. Uniform foams with densities below 1 g/cm^3 could be obtained.
- Foaming is very sensitive to the properties of the lead powder used. Dry and fluid powder with a grain size of ≈80 μm and a moderate oxygen content (≈ 0.2 wt.%) was the best choice.
- Basic lead(II) carbonate $(PbCO_3)_2{\cdot}Pb(OH)_2$ was shown to be a suitable blowing agent.

- Powder mixtures have to be densified by extrusion and can then be foamed ideally at 450°C.
- The foaming of lead and lead alloys is governed by the same parameters known to influence foaming of aluminium alloys. Foaming temperature and alloy composition are the most important ones.
- Pb-Sn alloys are found to reach higher foam expansions and show an increased foam stability as compared to pure lead. Pb-Sb alloys are more prone to foam collapse and drainage. Ternary alloys containing both Sb and Sn behave similar to Pb-Sn foams, i.e. expand more and are more stable than pure lead foams.
- Reasons for the beneficial action of tin are the positive influence on powder compaction and the early formation of a liquid phase during heating to the foaming temperature.

Acknowledgements

The work was supported financially by DLR (contract 50 WM 9821 and 50 WM 0126) and ESA (14308/00/NL/SH). Peter Weferling carried out some preliminary tests on different lead powders. Accumulatorenwerke Hoppecke Brilon supported some of the early work on lead foams.

References

[1] J. Banhart. Prog Mater Sci 2001;46:559

[2] J. Baumeister. Verfahren zur Herstellung poröser Metallkörper. 1990; German Patent 40 18 360

[3] B.C. Allen, M.W. Mote, A.M. Sabroff. Method of making foamed metal. 1963; US Patent 3,087,807

[4] F. Baumgärtner, I. Duarte, J. Banhart. Adv Eng Mater 2000;2:168

[5] M.F. Ashby, A. Evans, N.A. Fleck, L.J. Gibson, J.W. Hutchinson, H.N.G. Wadley. Metal foams – a design guide. London: Butterworth-Heinemann, 2000

[6] H.P. Degischer, B. Kriszt, editors. Handbook of Cellular Metals, Weinheim: Wiley-VCH, 2002

[7] H. Koch, T. Burkhardt. Untersuchungen der supraleitenden Eigenschaften geschäumter Bleiproben. 2000; Technical Report, University of Jena (Germany)

[8] T. Wübben, H. Stanzick, J. Banhart, S. Odenbach. J. Phys: Condensed Matter 2003;15:S427

[9] J. Banhart. Verfahren zur Herstellung poröser Metallkörper und Verwendung derselben. 2001; German Patent 101 15 230

[10] J. P. Hilger. J Power Sources 1995;53:45

[11] D.R. Lide (Ed.). Handbook of Chemistry and Physics, 85th edition. Boca Raton: CRC Press, 2004

[12] F. von Zeppelin, M. Hirscher, H. Stanzick, J. Banhart. Composite Science and Technology 2003;63:2293

[13] I. Duarte, J. Banhart. Acta Mater 2000;48:2349

[14] P. Weferling. Optimierung der Herstellungsparameter von Bleischaum. 1999; Diploma thesis, Hochschule Bremen (Germany)

[15] T. Wübben. Zur Stabilität flüssiger Metallschäume. Fortschrittsberichte Series 3, No. 803. Düsseldorf : VDI-Verlag, 2004

[16] J. Banhart. Journal of Metals 2000;52:22

[17] S.W. Ip, Y. Wang, J.M. Toguri., Canadian Metallurgical Quarterly 1999;38:81

[18] V. Gergely, T.W. Clyne. Adv Eng Mater 2000;2:175

[19] N. Babcsán, D. Leitmeier, H.P. Degischer, J. Banhart. Adv Eng Mater 2004;6:421

[20] B.P. Binks. Curr. Opin. Colloid Interface Sci 2002;7:21

[21] G. Kaptay. Colloids and Surfaces A 2004;230:67

[22] P. Weigand. Thesis, University of Aachen, 1999

[23] www.matweb.com

[24] B. Matijasevic-Lux, A. Rack, A. Haibel, J. Banhart. Influence of Powder Pre-Treatments on Metal Foam Pore Structure. In: R.F. Singer, C. Körner, V. Altstädt, H. Münstedt, editors. Cellular Metals and Polymers 2004. Uetikon-Zurich (CH): Transtech Publications, 2005, p. 57.

[25] D. Lehmhus, G. Rausch. Adv Eng Mater 2004;6:313

[26] H. Stanzick, I. Duarte, J. Banhart. Materialwissenschaft und Werkstofftechnik 2000;31:409

[27] H. Stanzick, M. Wichmann, J. Weise, J. Banhart, L. Helfen, T. Baumbach. Adv Eng Mater 2002;4:814

[28] C. Körner, M. Arnold, R.F. Singer. Mat Sci Eng A 2005;396:28

Figures & Tables

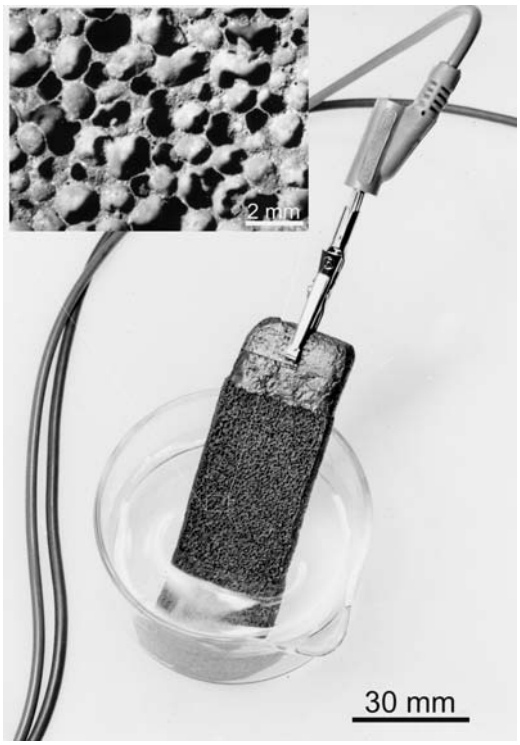

Figure 1. Application example for lead foam: conductive electrode grid in a lead-acid battery, inset: magnified view of a foam section cut by EDM (pure lead, foamed with 2 wt.% $(PbCO_3)_2 \cdot Pb(OH)_2$ at 450°C).

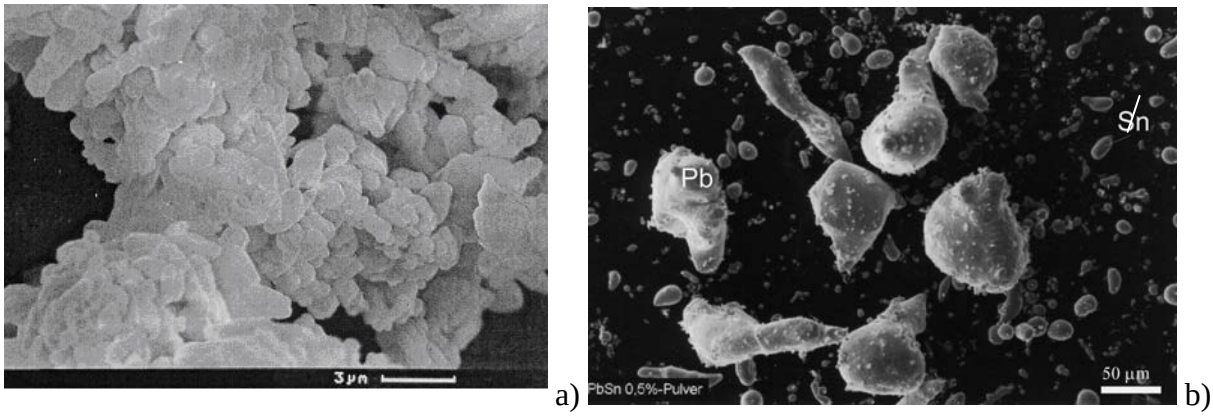

a) b)

Figure 2. a) $(PbCO_3)_2 \cdot Pb(OH)_2$ powder used as blowing agent, b) lead powder (large particles) mixed with 5% tin powder (small round particles) and 0.5 wt.% of $(PbCO_3)_2 \cdot Pb(OH)_2$ (tiny particles on top of Pb). Both images are obtained using a SEM operated at 20 keV.

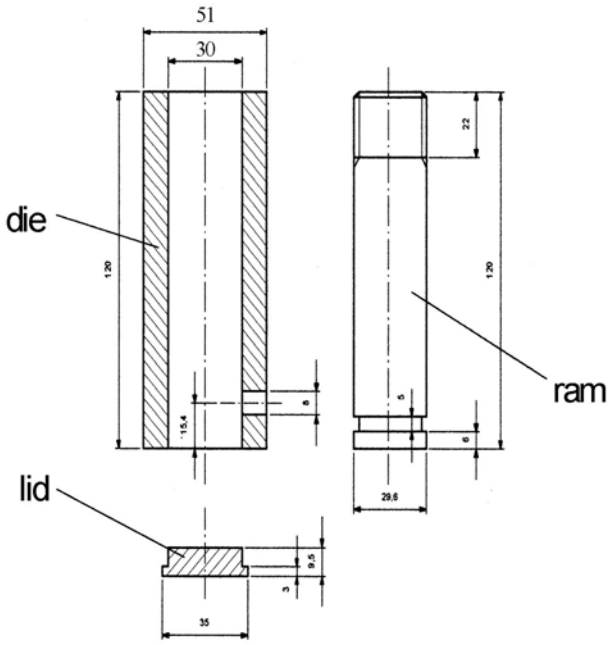

Figure 3. Tool used for lead powder extrusion.

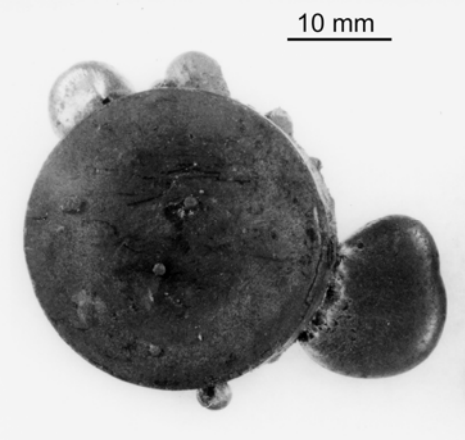

Figure 4. Top view of hot-pressed precursor sample heated to 450°C. No foaming was observed but liquid lead was squeezed out of tablet.

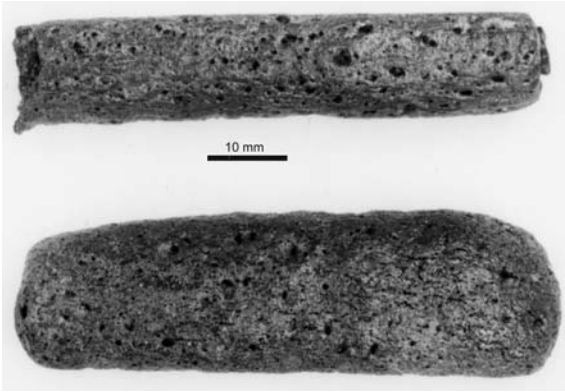

Figure 5. Lead foams produced at 400°C (upper) and 500°C (lower). 8 mm thick extruded wires containing 2 wt.% $(PbCO_3)_2 \cdot Pb(OH)_2$ were used as precursors.

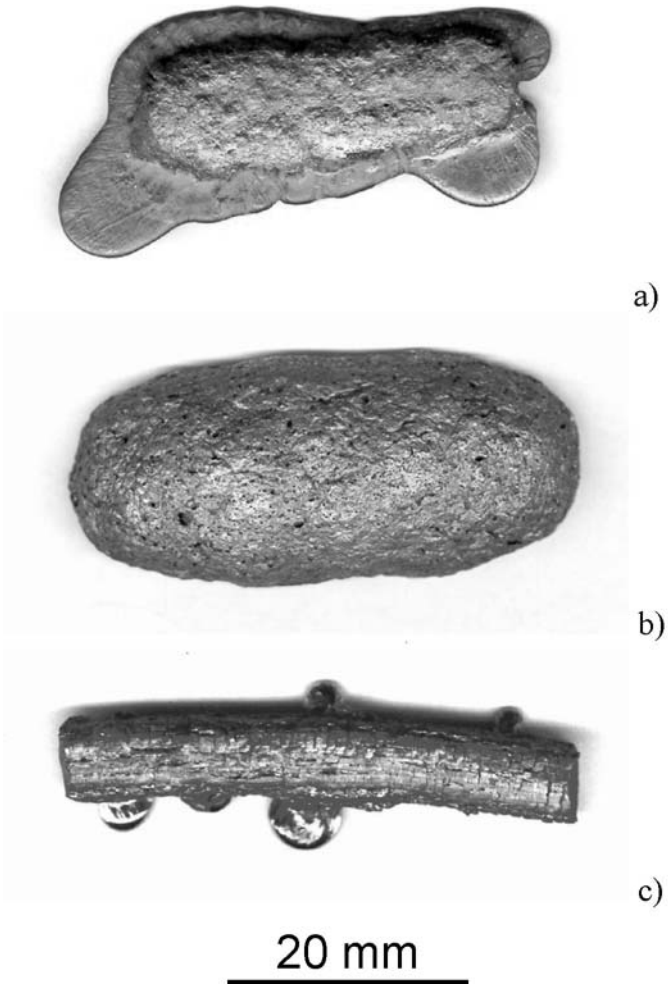

Figure 6. Foams prepared from three different powders [16], a) Chempur lead shot with 0.06 wt.% oxygen, b) Cerac-Chemco powder with 0.16 wt.% oxygen, c) Chempur powder with 1.21 wt.% oxygen.

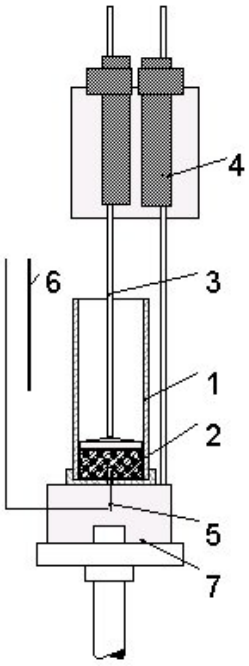

Figure 7. Set-up of mechanical “expandometer” for measuring foaming kinetics. 1: steel tube, 2: foamable precursor, 3: piston, 4: position sensor, 5: thermocouple for sample, 6: thermocouple for furnace, 7: sample support.

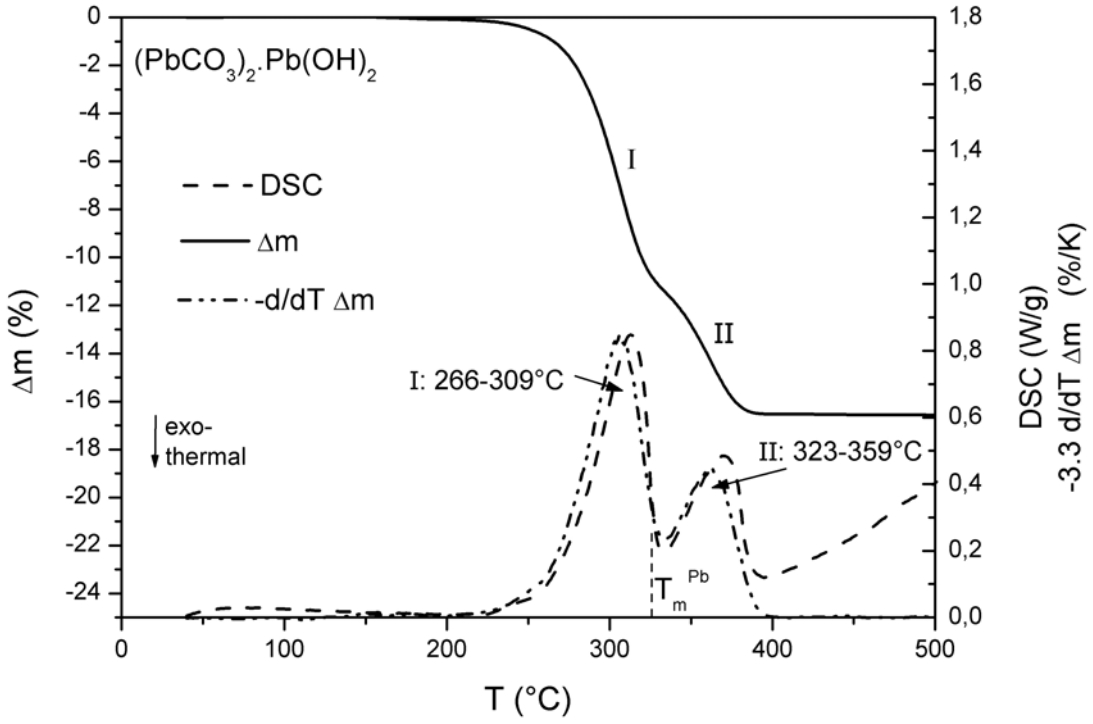

Figure 8. DSC and TGA trace of blowing agent $(PbCO_3)_2 \cdot Pb(OH)_2$. Heating rate 10 K/min, argon atmosphere. Mass change Δm (TGA), negative derivative of Δm and heat flow (DSC) are shown. The scale of –d/dT Δm was chosen such that the height of the first peak matched the corresponding DSC peak. Vertical line: melting point of lead.

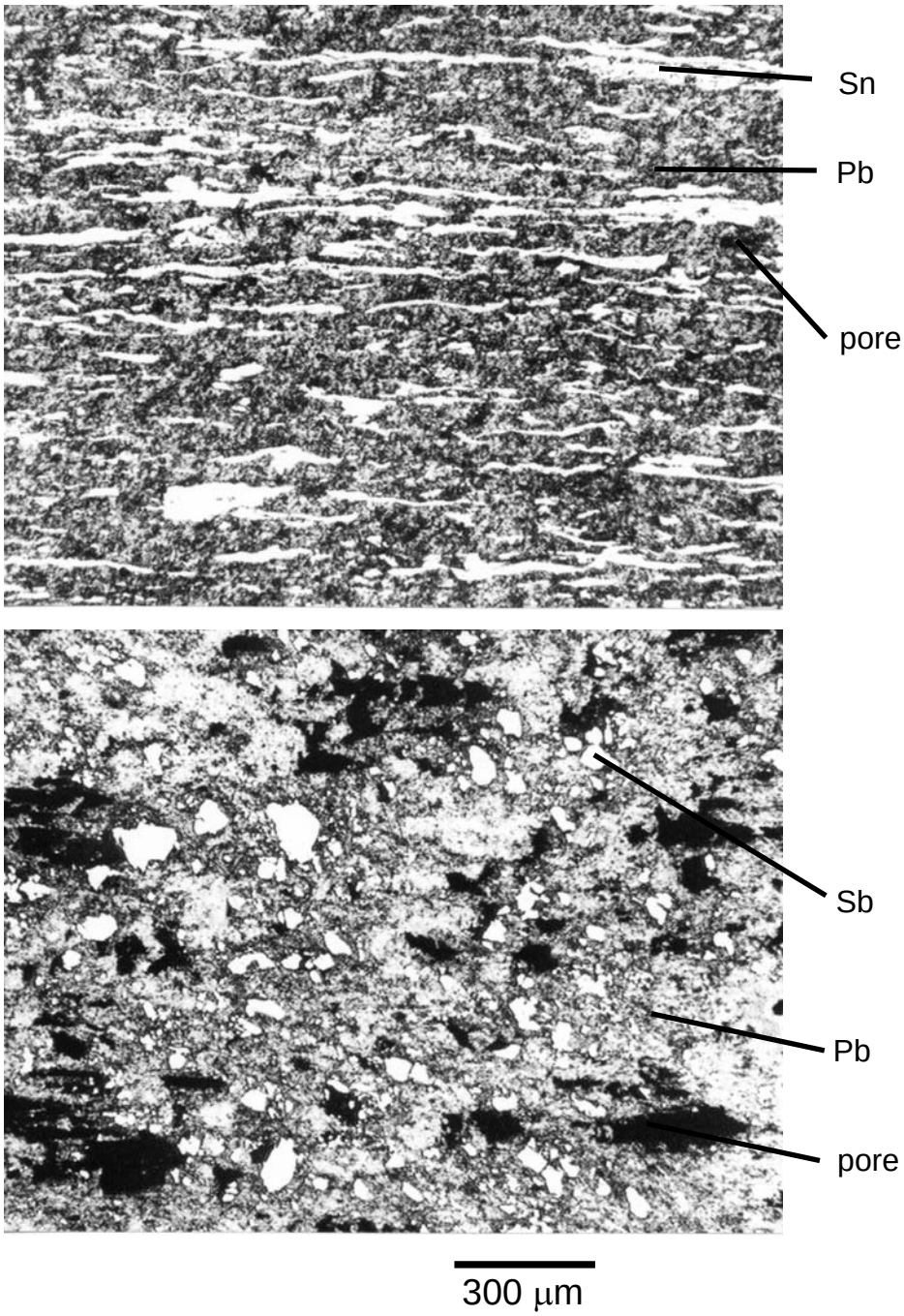

Figure 9. Sections of cold rolled a) PbSn10 b) PbSb10 precursor material containing 2 wt.% $(PbCO_3)_2 \cdot Pb(OH)_2$ (optical microscopy) .

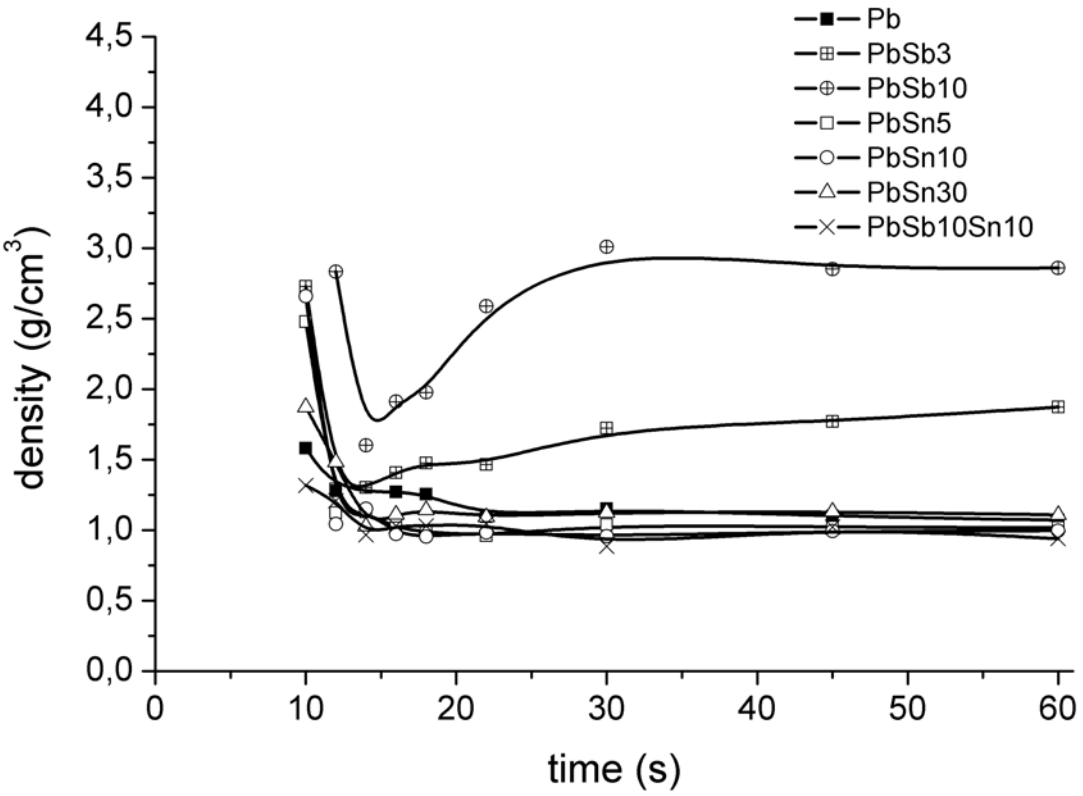

Figure 10. Density of various lead and lead alloy foams as a function of foaming time. 7 different alloys were investigated. All samples contained 2 wt.% $(PbCO_3)_2 \cdot Pb(OH)_2$. Foaming temperature was 450°C. t=0 corresponds to the first contact of the precursor with the pre-heated substrate. Data points are connected by guidelines to visualise the general course of foaming.

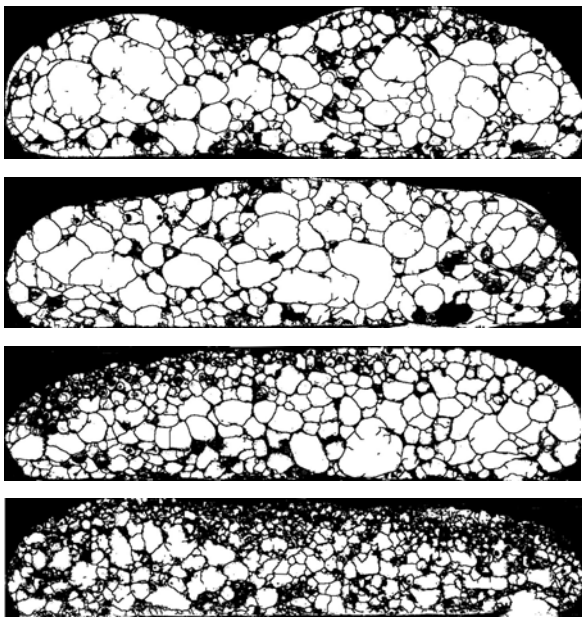

Figure 11. Sequence of foaming steps in PbSb10Sn10 containing 2 wt.% $(PbCO_3)_2 \cdot Pb(OH)_2$. Foaming temperature was 450°C. Density ρ and mean apparent pore diameter *d* are given.

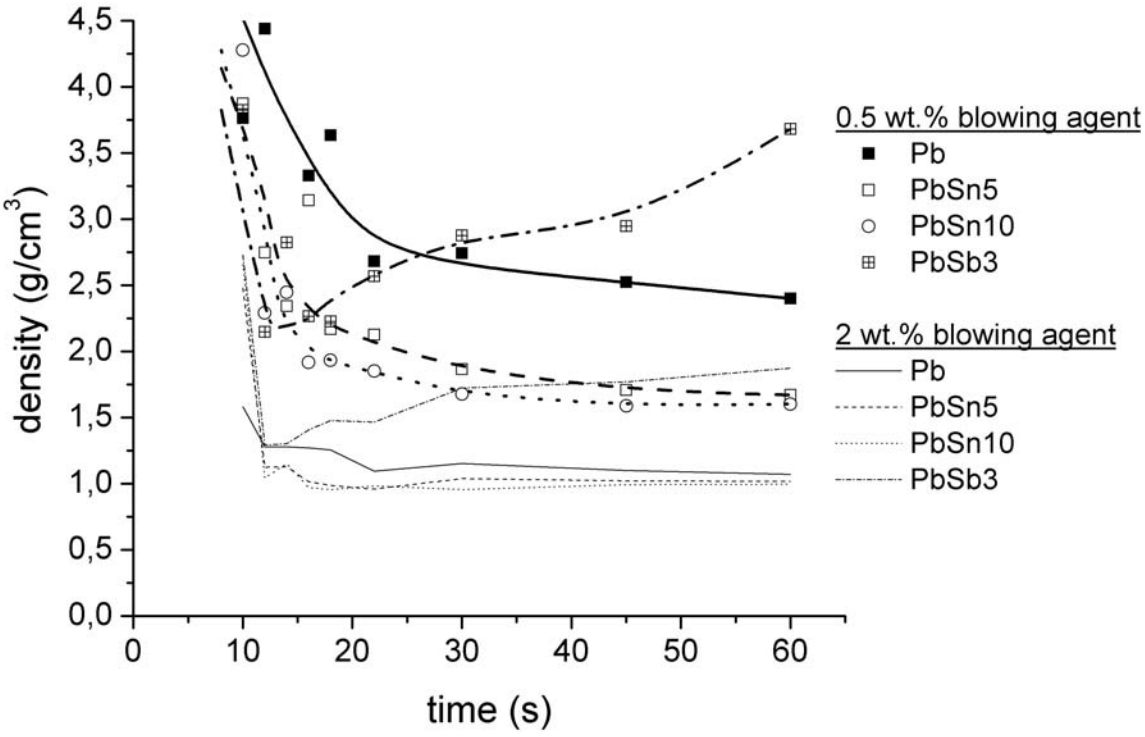

Figure 12. Density of various lead and lead alloy foams as a function of foaming time. Comparison of blowing agent contents: 0.5 and 2 wt.% $(PbCO_3)_2 \cdot Pb(OH)_2$. Foaming temperature was 450°C. Curves for 2% blowing agent as given in Figure 10 are represented by thin lines. Data points for 0.5 wt.% blowing agent are connected by guidelines to visualise the general course of foaming.

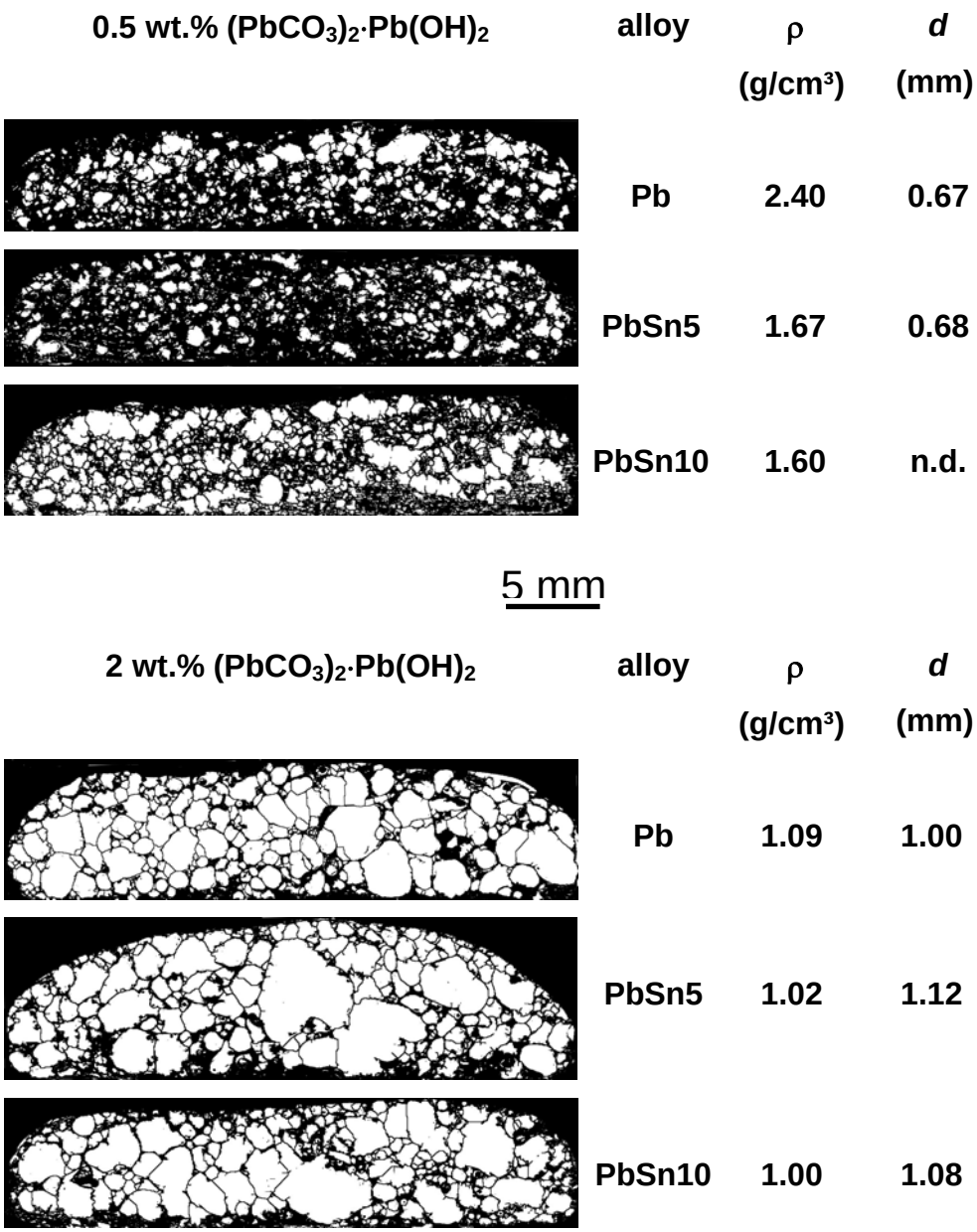

Figure 13. Pore morphology of foams after 60 s of foaming at 450°C. Two different contents of blowing agent: upper: 0.5 wt.%, lower: 2 wt.%. Densities ρ and mean apparent pore diameters *d* are given.

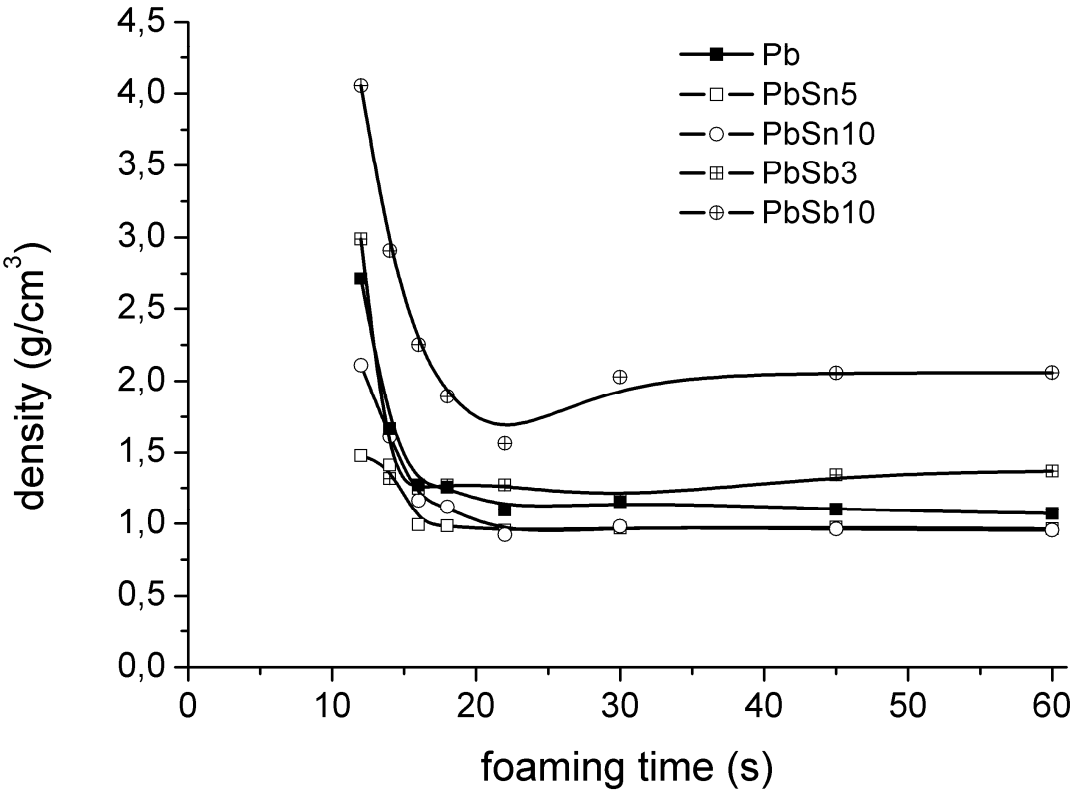

Figure 14. same as Figure 10 for foaming temperature 400°C.

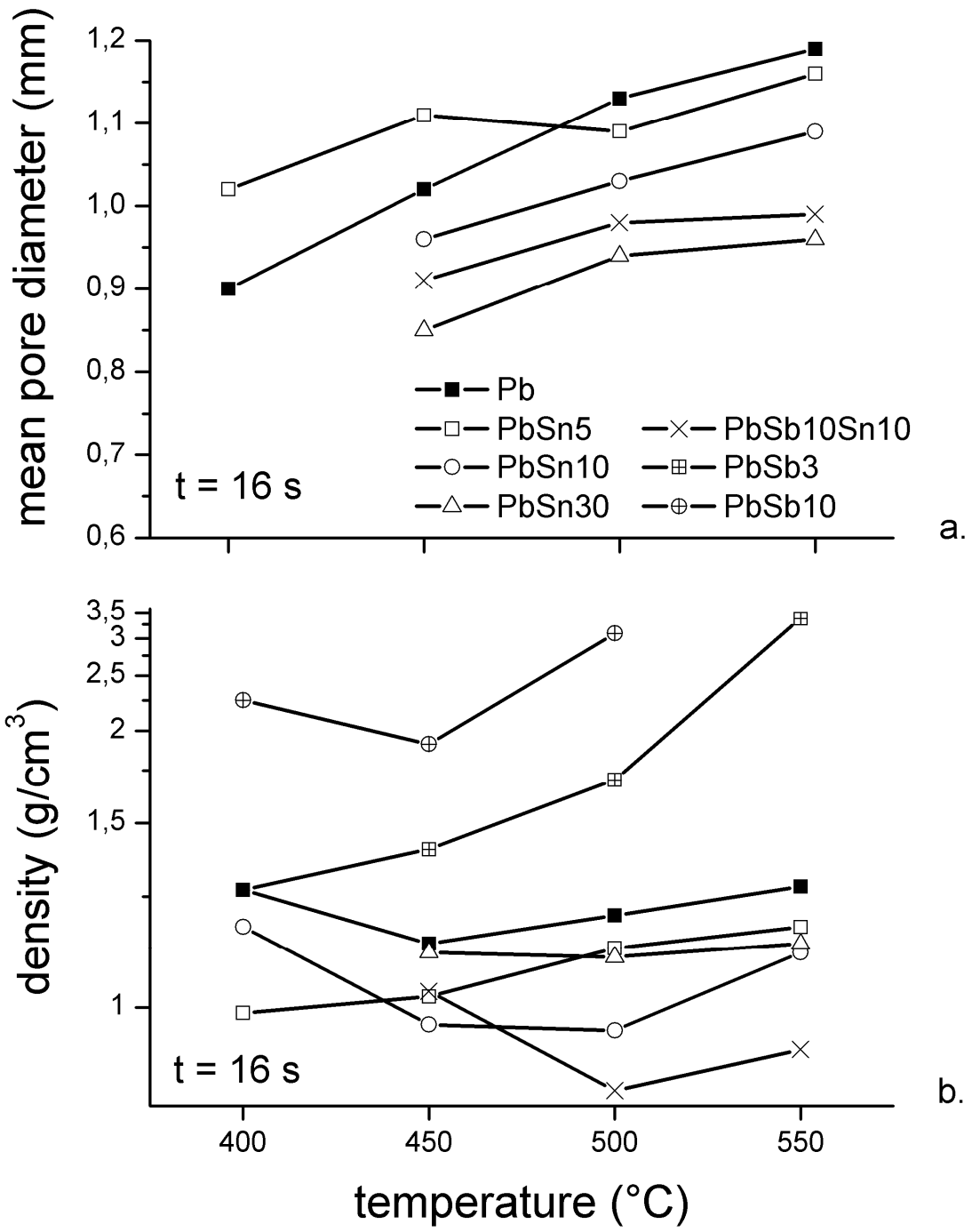

Figure 15. a) Mean apparent pore diameter of samples and, b) density of samples foamed at different temperatures for 16 seconds (2 wt.% $(PbCO_3)_2 \cdot Pb(OH)_2$).

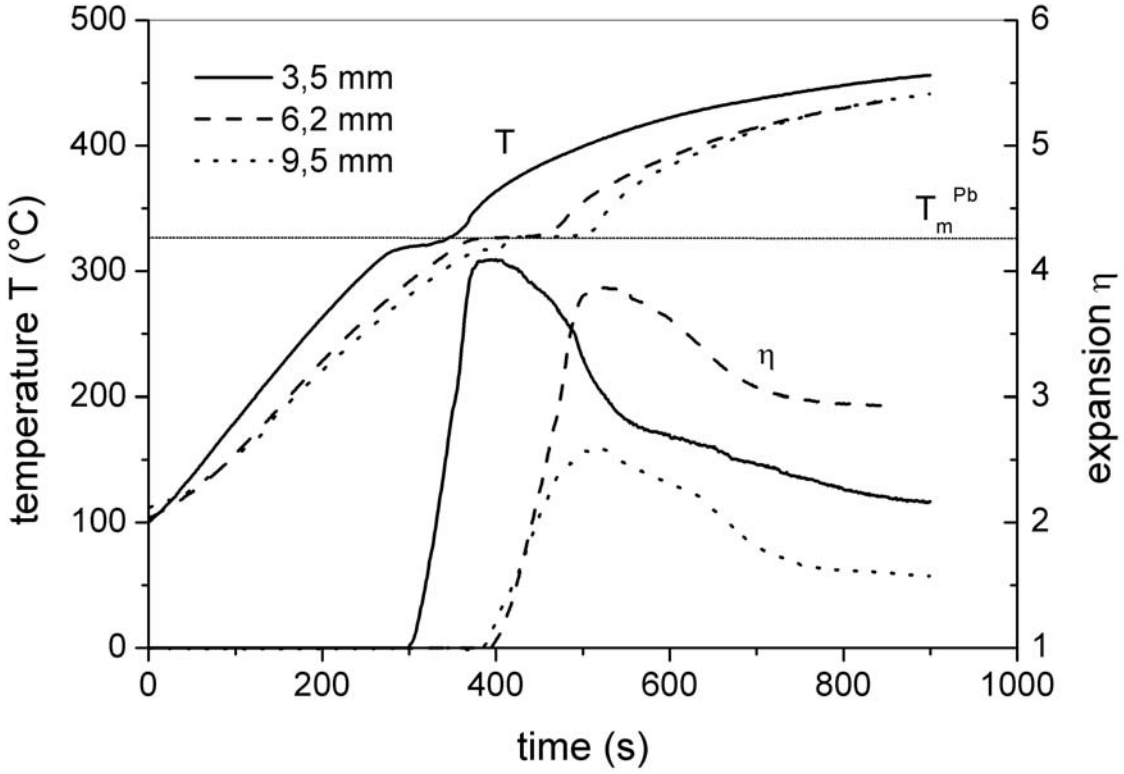

Figure 16. Expansion kinetics of pure lead precursor samples with three different thicknesses. Blowing agent: 2wt.% $(PbCO_3)_2 \cdot Pb(OH)_2$, furnace temperature 450°C.

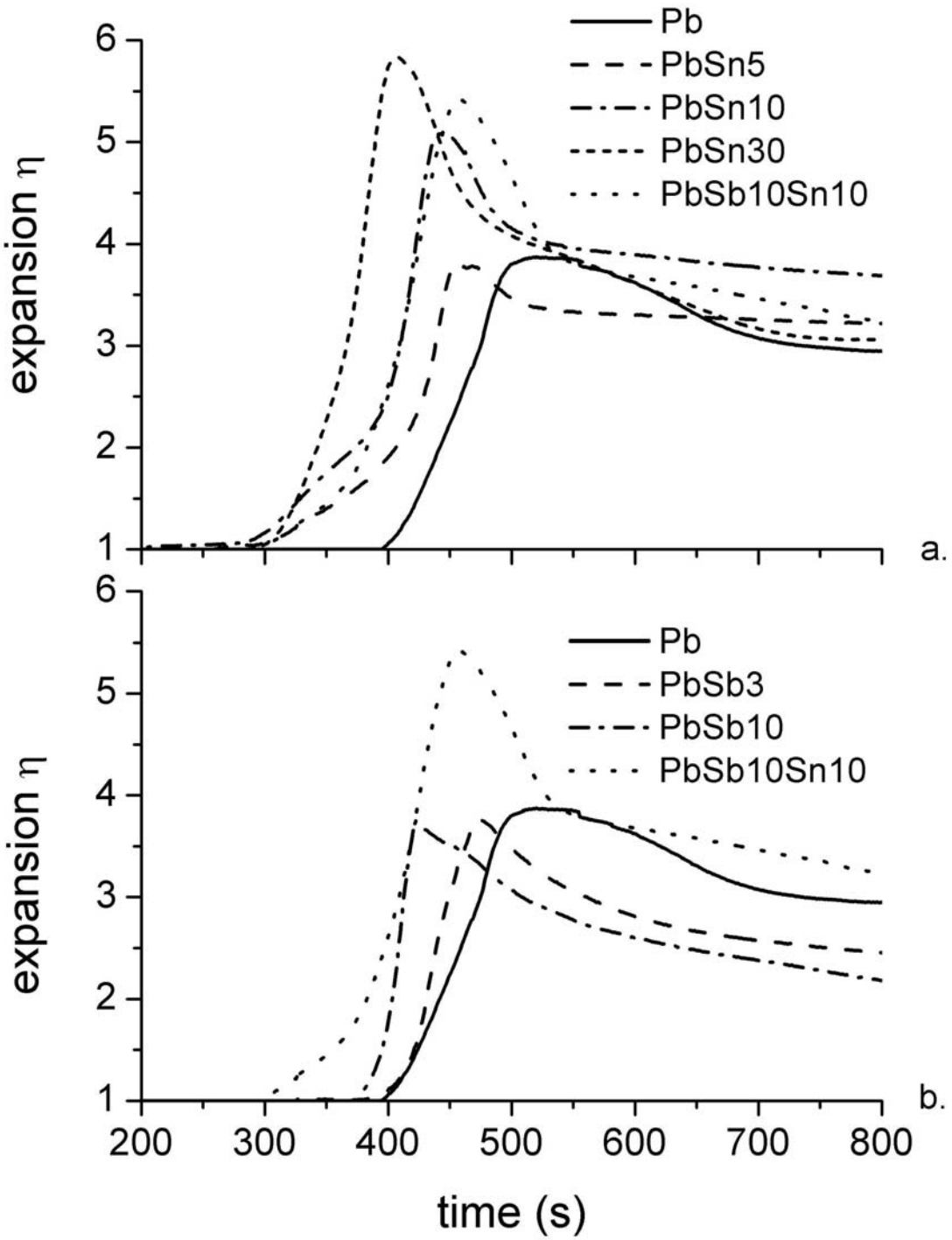

Figure 17. Expansion kinetics of pure lead and some alloys containing a) Sn and b) Sb. Blowing agent: 2wt.% $(PbCO_3)_2 \cdot Pb(OH)_2$, furnace temperature 450°C.

Table 1: Properties of the various lead powders evaluated. Properties given by the manufacturer are marked by an asterisk, all others were measured by the authors (n.d.=not determined). Bold writing indicates the powder finally selected as the best. The entries are sorted by increasing "foaminess" (term explained in Sec. 2.2.4).

manufacturer	**product type***	**particle size spectrum* (µm)**	**purity* (%)**	**mean particle size (µm)**	**oxygen content (wt.%)**	**equivalent PbO content (vol.%)**	**foaminess (%)**
Goodfellow	powder	< 150	99.5	56	2.86	47	0
ALFA	powder	< 75	99	n.d.	4.11	65	0
Chempur	powder	< 150	99.5	n.d.	1.21	21	20
ALFA	powder	< 150	99.5	9	1.01	17	23
Aldrich	shot	<500	99.9	n.d.	0.27	5	37
Chempur	shot	400-800	99.9	n.d.	0.06	1	37
Eckart	powder	< 63	99.5	9	0.15	3	43
Goodfellow	powder	75-180	99.9	148	0.23	4	47
Riedel de Haen	granulate	<800	„pure“	n.d.	0.03	0.5	50
ALFA	powder	< 150	99.5	55	0.09	1.6	70
ABCR	powder	<150	99.5	59	0.46	8	80
Chemco/Cerac	**powder**	**44-105**	**99.9**	**82**	**0.12 (0.16)**	**2 (3)**	**93**

Table 2. Quality assessment of lead foams. The four properties given in the left column were valued with up to three points each which were then first weighted with the factor given in column 2 and then summed up a total quality number. A "foaminess" is the defined as the percentage of the possible 30 points which is actually reached (explained in Sec. 2.2.4 and given in Table 1).

foam property	**weight factor**	**points**			
		0	**1**	**2**	**3**
surface quality	1	very jagged	uneven, many holes	some defects	smooth and closed
pore structure	4	no pores	mainly open porosity	closed pores, but irregular	closed pores, uniform size
expansion factor	3	<1	>1 <2	>2 <3	>3
strength of foam	2	very fragile	low	medium	high